Electrochimica Acta, 1972, Vol. 17, pp. 2153 to 2179. Pergamon Press. Printed in Northern Ireland

THE ANODIC OXIDATION OF THIOCYANATE ION DISSOLVED AS KSCN IN DIMETHYL-SULPHOXIDE*

C. MARTINEZ, A. J. CALANDRA and A. J. ARVÍA
Instituto de Investigaciones Fisicoquímicas Teóricas y Aplicadas, División Electroquímica, Facultad de Ciencias Exactas, Universidad Nacional de La Plata, La Plata, Argentina

Abstract—The anodic oxidation of SCN^- ion dissolved as KSCN in dimethylsulphoxide, on platinum electrodes, was investigated at *ca* 25, 60 and 160°C by means of various non-stationary electrochemical techniques. At low temperatures one anodic and two main cathodic processes were found. The anodic oxidation of SCN^- ion yields as primary product the SCN radical, which readily produces $(SCN)_2$. The latter can be in part reduced back to SCN^- ion, because it reacts in part yielding solvated hydrogen ions which cause the second cathodic reaction. In the region of 60°C, no $(SCN)_2$ cathodic current is observed. In the region of 160°C the only reaction is SCN^- ion oxidation and the primary product polymerizes to $(SCN)_x$, which forms a film on the electrode, causing passivation.

On the basis of kinetic data obtained for the different reactions, a mechanism for the anodic oxidation of the SCN^- ion and for the passivating film formation is suggested. The second process only partly fits the Müller model for the electrochemical growth of insoluble layers.

Résumé—Etude à 25, 60 et 160°C (environ) au moyen de diverses techniques électrochimiques non-stationnaires, de l'oxydation anodique de l'ion SCN^-, dissous en KSCN dans la diméthylsulfoxyde. Aux basses températures, un processus anodique et deux processus cathodiques principaux se manifestent. L'oxydation anodique de l'ion SCN^- engendre le radical SCN comme produit primaire, qui se transforme aisément en $(SCN)_2$. Réciproquement, ce dernier peut être réduit partiellement en ion SCN^-, parce qu'il peut réagir en produisant des ions hydrogène solvatés qui suscitent la seconde réaction cathodique. Au voisinage de 60°C, on n'observe aucun courant cathodique correspondant à $(SCN)_2$. Au voisinage de 160°C, la seule réaction est l'oxydation de l'ion SCN^- et le produit primaire se polymérise en $(SCN)_x$, qui forme un film passif sur l'électrode.

Sur la base des données cinétiques obtenues pour les différentes réactions, on suggère un mécanisme pour l'oxydation anodique de l'ion SCN^- et pour le formation du film passivant. Seul, le second processus satisfait au modèle de Müller, relatif à la croissance électrochimique des couches insolubles.

Zusammenfassung—Man untersuchte die anodische Oxydation von SCN^--Ionen, welche durch Auflösen von KSCN in DMSO erhalten wurden. Man arbeitete mit Platinelektroden bei 25, 60 und 160°C indem man verschiedene nicht-stationäre elektrochemische Arbeitsmethoden anwandte. Bei tiefen Temperaturen fand man einen anodischen und zwei kathodische Hauptprozesse. Die anodische Oxydation des SCN^--Ions ergibt als Primärprodukt ein SCN-Radikal, welches leicht $(SCN)_2$ bildet. Dieses kann teilweise zum SCN^--Ion reduziert werden, weil es teilweise unter Bildung von solvatisierten Wasserstoffionen reagiert, welche die zweite kathodische Reaktion bewirken. Bei 60°C wird kein kathodischer $(SCN)_2$-Strom beobachtet. Bei 160°C ist die Oxydation des SCN^--Ions die einzige Reaktion. Das entstehende Produkt polimerisiert zu $(SCN)_x$, das auf der Elektrodenoberfläche einen Film bildet, welcher zu einer Passivierung der Elektrode führt. Aufgrund der kinetischen Daten, welche für die verschiedenen Reaktionen erhalten wurden, wird ein Mechanismus für die anodische Oxydation des SCN^--Ions und für die Bildung des passivierenden Films vorgeschlagen. Der zweite Vorgang erfüllt nur teilweise das Modell von Müller für das elektrochemische Wachstum von unlöslichen Oberflächenschichten.

INTRODUCTION

SEVERAL authors[1–3] have considered the electrochemical oxidation of the SCN^- ion in aqueous media, establishing that the product of the initial reaction is probably the radical SCN or thiocyanogen $(SCN)_2$. As neither of these is stable in water, the total reaction forms HCN according to

$$SCN^- + 4\,H_2O \rightarrow SO_4^{2-} + HCN + 7\,H^+ + 6\,e.$$

The oxidation of thiocyanate ion has also been studied from a preparative point of view, using organic solvents such as water-alcohol mixtures and acetonitrile.[4–5]

* Manuscript received 5 January 1972.

The products obtained are an indication that the product of the initial discharge of the SCN^- ion is the SCN radical.

The kinetics of the anodic oxidation of the SCN^- ion was recently investigated using acetonitrile (ACN) as solvent.[6-7] At temperatures lower than 0°C the pseudo-halogen electrode represented by the equilibrium

$$2\,SCN^- \rightleftarrows (SCN)_2 + 2\,e$$

was studied with cyclic voltammetry and a probable mechanism of reaction was postulated.[6]

The formation of parathiocyanogen, $(SCN)_x$, was observed at a temperature near the boiling point of the solvent[7] as an insoluble product on the electrode surface, because of the polymerization of the substance formed in the initial electrochemical reaction. The polymer formation was also found in the anodic discharge of the SCN^- ion using molten KSCN.[8,9] In both cases the study of this reaction was interesting as it was related to passivity theory.

The oxidation of the SCN^- ion can thus be studied under several experimental conditions, either by changing the medium composition or the temperature. Following this approach we have investigated the reaction using dimethylsulphoxide (DMSO) (mp 18·4°C, bp 189°C) as solvent. Highly concentrated KSCN solutions can be obtained in this solvent, giving the possibility of gathering sufficient kinetic information to try a mechanistic interpretation of the electrode reactions.

EXPERIMENTAL TECHNIQUE

Conventional electrolytic cells with three electrodes placed in separated compartments were used. The cell for experiments at room temperature was similar to that reported previously.[10]

For higher temperatures a cell was designed to avoid solvent elimination during the experiments. The working electrode was either a wire or a platinum disk of spectroscopic quality and these were polished to mirror surface before each experiment. The apparent working electrode area was between 0·07 and 0·8 cm^2. The counter-electrode was a platinum sheet with an area 100 times larger than the working-electrode area. As reference electrode a silver chloride electrode in 10^{-3} M NaCl and 1 M $KClO_4$ solution in DMSO was used. The solvent was purified following the procedure described in the literature.[10] Its residual water content was 0·03%. Two types of solutions were used, one without supporting electrolyte and either 2 M or 4 M KSCN concentration. The other was 1 M $KClO_4$ and the KSCN concentration was varied between 10^{-3} and 10^{-2} M. Analytical reagent chemicals previously vacuum-dried at about 100°C were employed. Current/potential curves were determined under non-stationary conditions by means of cyclic voltammetry at sweep rates between 1 and 170 mV/s.

The cyclic voltammetry was applied starting from the rest potential towards increasingly positive potentials (increasing half-cycle), reaching a maximum pre-fixed potential. In some experiments the initial potential, E_i, was located at more negative values than the rest potential. In some cases different potential-sweep rates were used for each half-cycle. The cyclic voltammetry was performed with and without compensation for ohmic resistance.

Potentiostatic runs were also made under quasi-stationary conditions. By means of galvanostatic reverse pulses, the potential relaxation for both the anodic and cathodic reactions was determined. The relaxation of the anodic current at constant potential was also analysed. A description of the measuring devices has been given elsewhere.[8,11] Runs were made at three temperature regions, 25, 60 and 160°C.

RESULTS

Cyclic voltammetry with solutions of high KSCN *concentration.*

Figure 1 shows several voltagrams obtained with a 2 M KSCN solution at 27°C. If the potential is swept at 10 mV/s up to 0·90 V referred to the initial potential, an

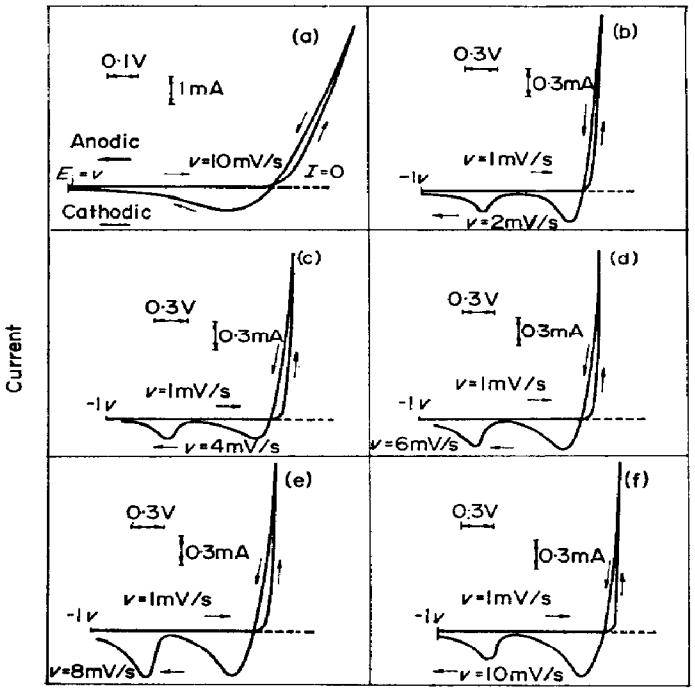

FIG. 1. Voltagrams obtained with a 2 M KSCN solution at 27°C.
a, v = 10 mV/s; b, c, d, e, v = 1 mV/s (positive half-cycle) and variable potential-sweep rate during the negative half-cycle.

anodic current appears when the potential exceeds 0·65 V. The current reaches 5 mA at the maximum potential. If the voltagrams are recorded at different potential-sweep rates for each half-cycle, with a higher rate for the decreasing half-cycle, the same current peaks are observed and their height ratio is independent of the potential-sweep rate. In the decreasing half-cycle a cathodic current peak occurs at about 0·5 V above the initial potential. If the potential sweep is initiated from a potential more negative than the initial one, such as −1·0 V, and this goes up to +0·9 V, the voltagram during the increasing half-cycle (at 1 mV/s) is the same to the one already described, while the voltagram during the decreasing half-cycle exhibits two cathodic current peaks with a separation of 0·820 ± 0·010 V. In these experiments the initial part of the return half-cycle shows, at constant potential, a higher current than that during

the increasing half-cycle. As the potential-sweep rate of the decreasing half-cycle is increased, the two cathodic current peaks shift toward more negative potentials. The height of the current peaks depends, at constant rate, on the sweep amplitude.

If the increasing potential sweep is made at 4 mV/s to reach a more positive pre-fixed potential, the tendency to the occurrence of an anodic current peak is observed (Fig. 2) and in the decreasing half-cycle recorded at 10 mV/s, the first cathodic current peak covers an area much greater than the second. This is an indication that a larger concentration of substance was formed anodically.

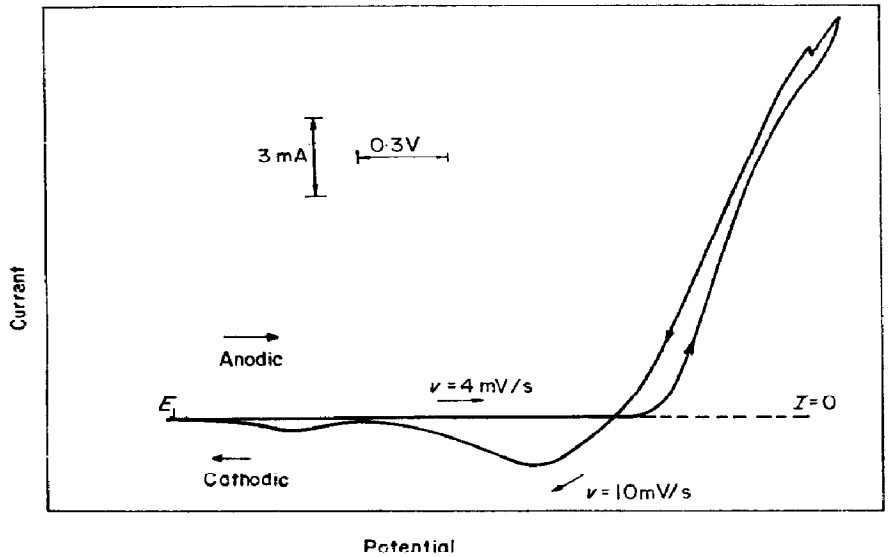

FIG. 2. Voltagrams obtained with a 2 M KSCN solution at 27°C. $v = 4$ mV/s (positive half-cycle) and $v = 10$ mV/s (negative half-cycle).

Voltagrams run at 60°C with the same solution from potentials more negative than the rest potential are different from those already described for lower temperature (Fig. 3). On the increasing half-cycle there is a tendency to establish an anodic current peak, and the first cathodic current peak observed at lower temperature no longer occurs. A cathodic current peak appears only at potentials more cathodic than the rest potential. The initial part of the decreasing half-cycle shows a hysteresis, contrary to that described at lower temperature. These results are confirmed by the galvanostatic experiments described further on.

At 157°C the voltagrams are different from those described at lower temperatures, as shown in Fig. 4. An anodic current peak located at positive potentials appears during the increasing half-cycle. Under these conditions the formation of a yellow-orange film on the electrode is observed. The electrochemical reduction of the anodic film, when the potential is swept towards potentials more negative than the rest potential, is not observed, but film detachment from the electrode occurs. The anodic current peak height, at sweep rates lower than 40 mV/s, depends linearly on the sweep rate (Fig. 5), while at higher rates it depends linearly on $v^{1/2}$. The parameters deduced from the voltagrams, including the height of the anodic peak, $I_{p,a}$, the potential at the current peak, E_p, and the charge used Q, (found by integrating the

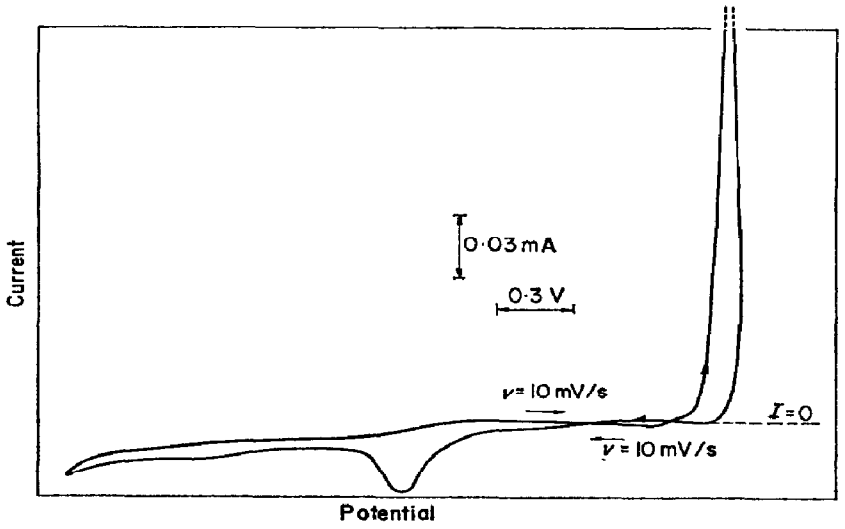

FIG. 3. Voltagram obtained at $v = 10$ mV/s with a 2 M KSCN solution at 66·5°C.

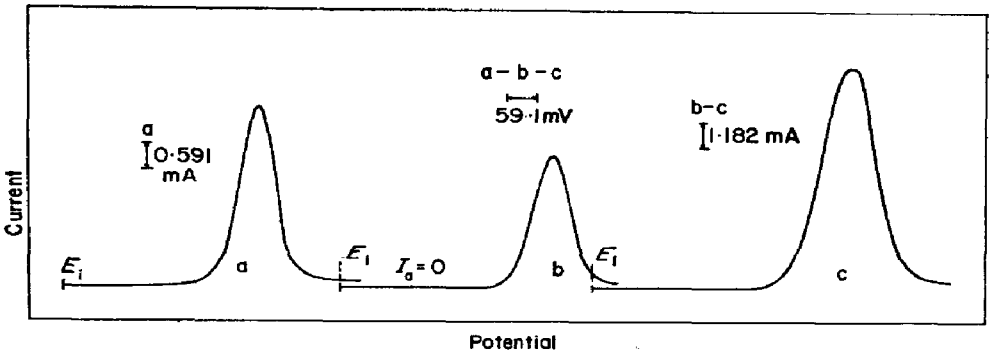

FIG. 4. Voltagrams obtained at different potential-sweep rates.
2 M KSCN solution, 157°C. Ohmic resistance, 3 Ω.

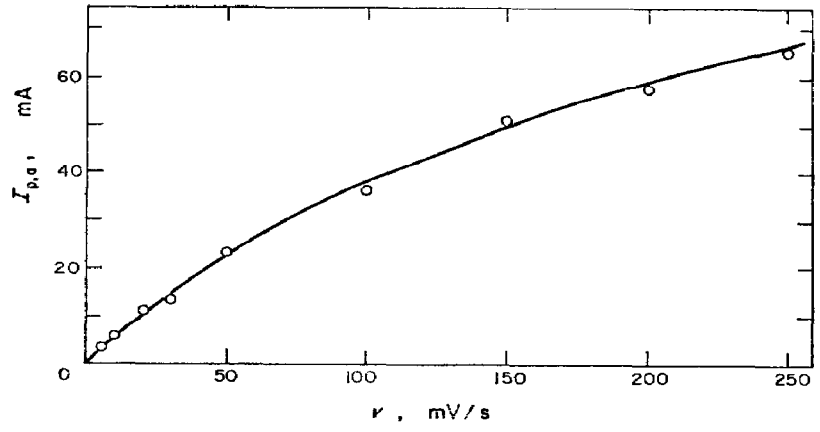

FIG. 5. Dependence of the anodic current peak on the potential-sweep rate.
2 M KSCN solution, 160°C. Ohmic resistance, 9 Ω.

TABLE 1. DATA FROM VOLTAGRAMS
157°C, 2 M KSCN

v mV/s	$I_{p,a}$ mA	$i_{p,a}$ mA/cm²	E_p V	Q mC/cm²
5	3·61	28·6	0·421	516
10	5·56	44·1	0·467	492
20	11·48	91·1	0·538	708
50	24·02	109·6	0·667	708
100	35·95	285·3	0·780	1020
200	57·75	458·3	0·935	1240

$R_{ohm} = 9{\cdot}0\ \Omega$.

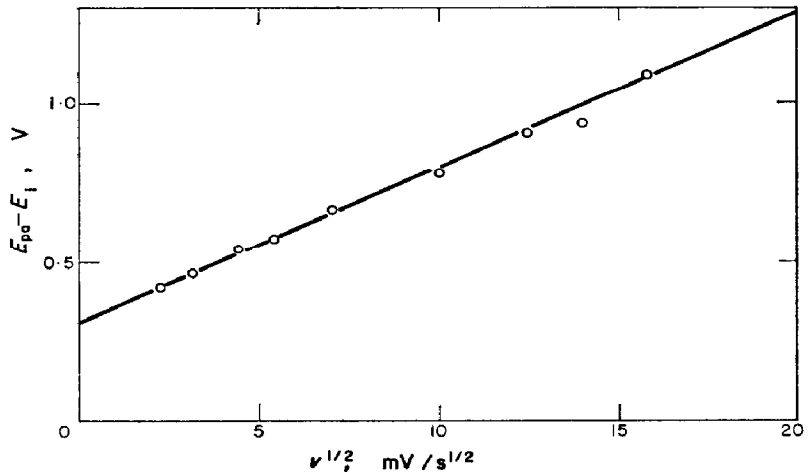

FIG. 6. Dependence of the potential related to the anodic current peak on the potential sweep rate.
2 M KSCN solution, 160°C. Ohmic resistance, 9 Ω.

curve) are indicated in Table 1. The potential of the anodic current peak depends linearly on $v^{1/2}$, when the ohmic resistance is sufficiently high (Fig. 6).

The voltagrams obtained with compensation for ohmic resistance have no distortions and the relationship between E_p and v can be established without any ambiguity, as seen in Figs. 7 and 8. Comparing the values of $I_{p,a}$/area of Tables 1 and 2 we conclude that the ohmic resistance has little influence, especially at low potential-sweep rates. In these experiments a clear relationship between E_p and log v is established (Fig. 9). In the velocity range investigated the straight line has a slope very close to $2{\cdot}3(2RT/3F)$ V/decade. Integration of the areas of the anodic peaks yields the charge Q that is concerned in the film formation. Values of Q appear in Table 2. They increase with the potential-sweep rate from 249 mC/cm², for the lower values of v, up to 1080 mC/cm² for the higher. For v lower than 20 mV/s, the anodic peak height depends linearly on v (Fig. 10). For v higher than 40 mV/s, a similar relationship is also obtained, but with a larger slope.

Galvanostatic pulses with concentrated KSCN *solutions.*

These experiments were performed at 27, 70 and 162°C with a 2 M KSCN solution. Results are given in Figs. 11, 12 and 13 for different conditions. Electrodes recently

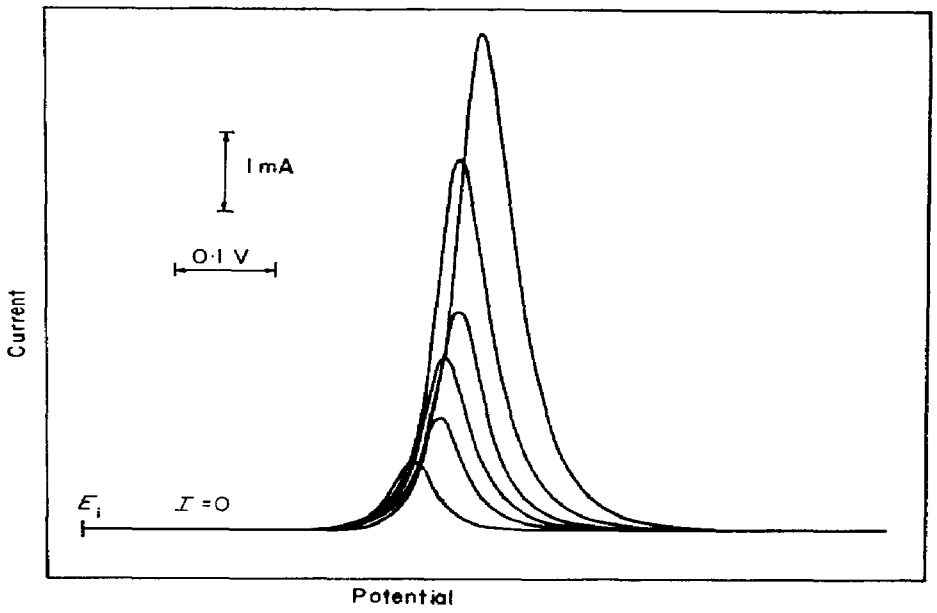

FIG. 7. Voltagrams obtained at different potential-sweep rates with ohmic resistance compensation.
4 M KSCN solution, 152°C.

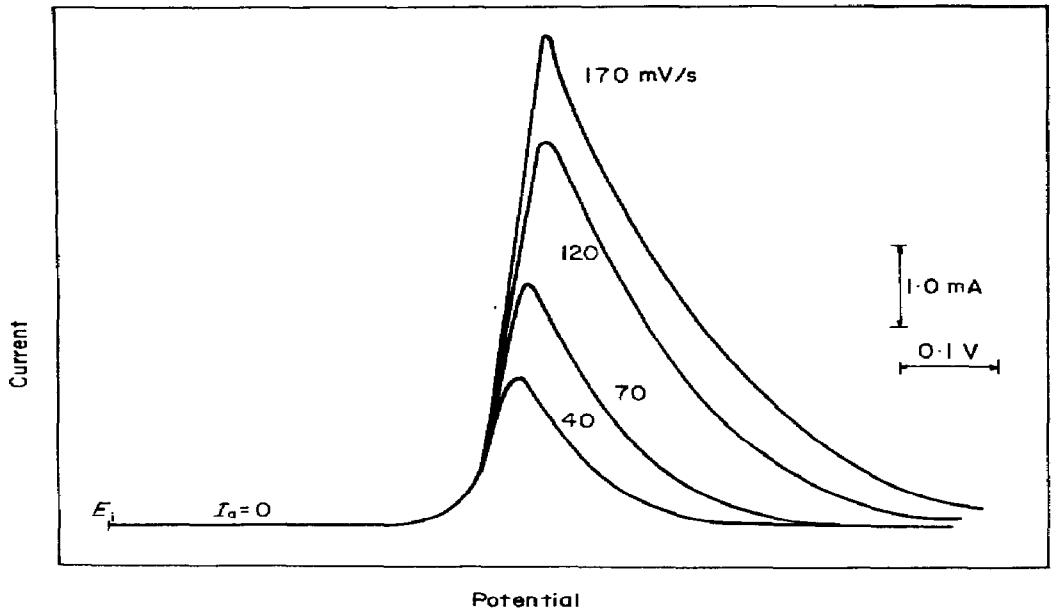

FIG. 8. Voltagrams obtained at different potential-sweep rates with ohmic resistance compensation.
4 M KSCN solution, 152°C.

TABLE 2. DATA FROM VOLTAGRAMS WITH OHMIC COMPENSATION
152°C, 4 M KSCN

v mV/s	$I_{p,a}$ mA	$i_{p,a}$ mA/cm²	E_p V	Q mC/cm²
3	0·7	11·1	0·332	505
7·5	2·3	36·5	0·365	700
15	4·6	73·0	0·383	802
20	6·0	92·6	0·400	824
40	18·0	286	0·419	1478
70	29·7	471	0·425	1710
120	48·0	762	0·438	2185
170	62·3	989	0·450	2185

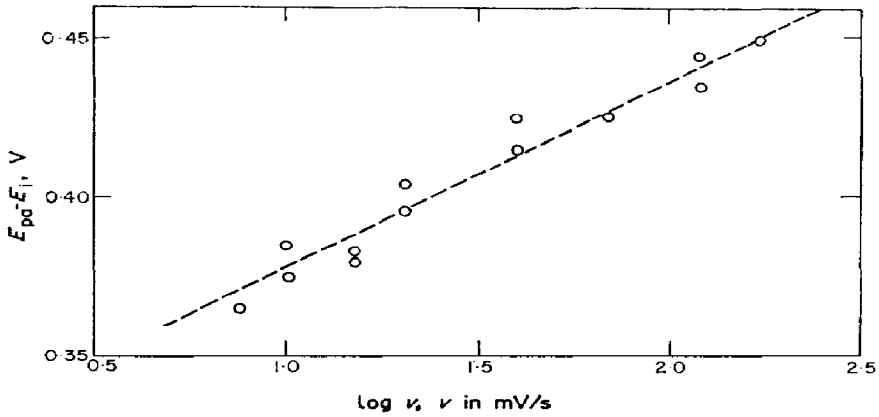

FIG. 9. Semilogarithmic plot of the potential of the anodic current peak *vs* the potential-sweep rate.
4 M KSCN solution, 152°C.

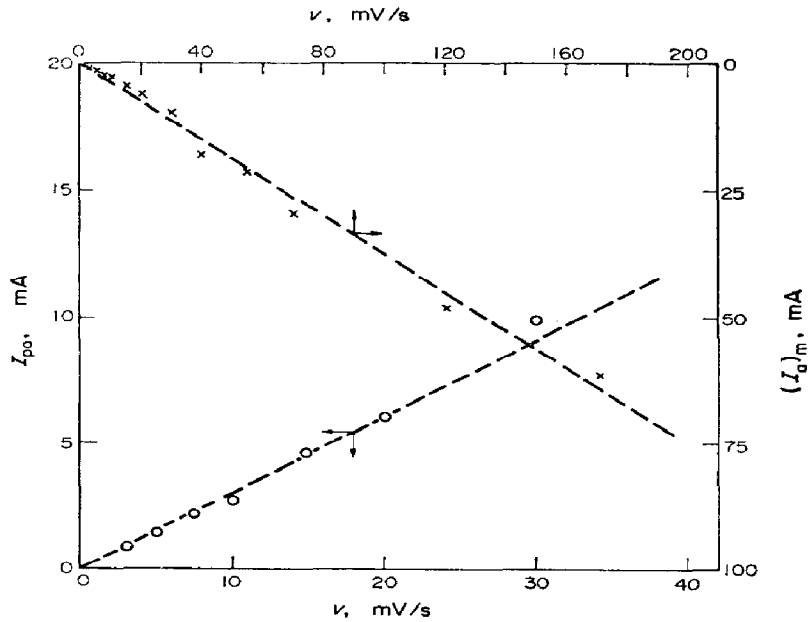

FIG. 10. Dependence of the anodic current peak on the potential-sweep rate.
4 M KSCN solution, 152°C.

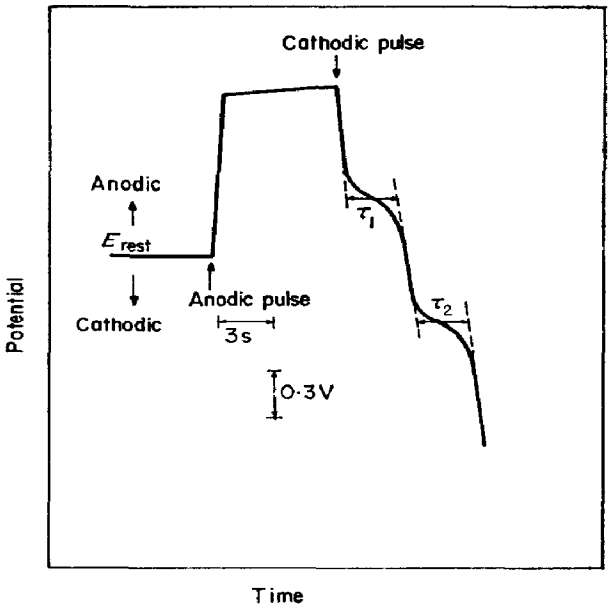

FIG. 11. Time dependence of the electrode potential when double current pulses (anodic and cathodic) are applied.
2 M KSCN solution, 27°C.

cleaned and polished before each run were used. Each galvanostatic record was initiated by applying first an anodic pulse; once a constant potential was attained, a cathodic pulse was applied, reaching a potential more negative than the initial rest potential of the system. No transition time was found in the potential/time curve during the anodic pulse at 27°C (Fig. 11), but during the cathodic pulse two transition times were observed, τ_1 and τ_2. The first occurs at potentials more positive than the rest potential and the second at potentials more negative. Data obtained from these experiments are assembled in Table 3. The subindex c corresponds to cathodic pulses and a to anodic.

The ratios $I_c\tau_1^{1/2}/Q_a$ and $I_c[(\tau_1 + \tau_2)^{1/2} - \tau_1^{1/2}]/Q_a$ are also included in Table 3, I_c being cathodic galvanostatic current pulse and Q_a the charge during the anodic galvanostatic pulse. The average values of these ratios, Table 3, are about 2. The products $I\tau^{1/2}$ belong to two independent cathodic processes, it being impossible at this moment to decide about their reversibility.

After repetitive galvanostatic experiments at 27°C the solution acquired a yellow colour.

Experiments at 70°C (Fig. 12) present no anodic transition time and during the cathodic pulse only the transition time τ_2 appears at negative potentials. Results obtained of 70°C are shown in Table 4, and are not very different from those obtained at lower temperatures; after some minutes of anodic electrolysis, a yellow-solid substance with little adherence appeared on the electrode.

At 162°C (Fig. 13) a net anodic transition time τ_2 appears and the electrode is covered with an insoluble yellowish film. The charge Q_a in this case varies between

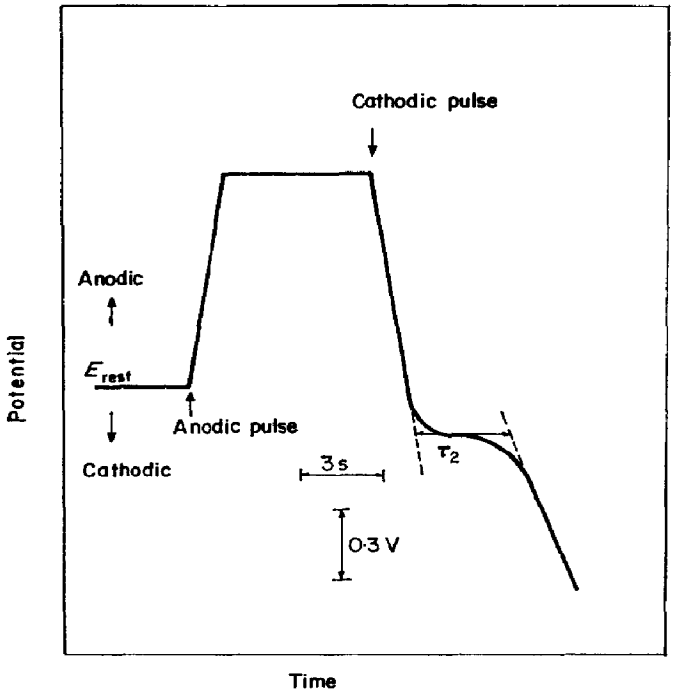

FIG. 12. Time dependence of the electrode potential when double current pulses (anodic and cathodic) are applied.
2 M KSCN solution, 70°C.

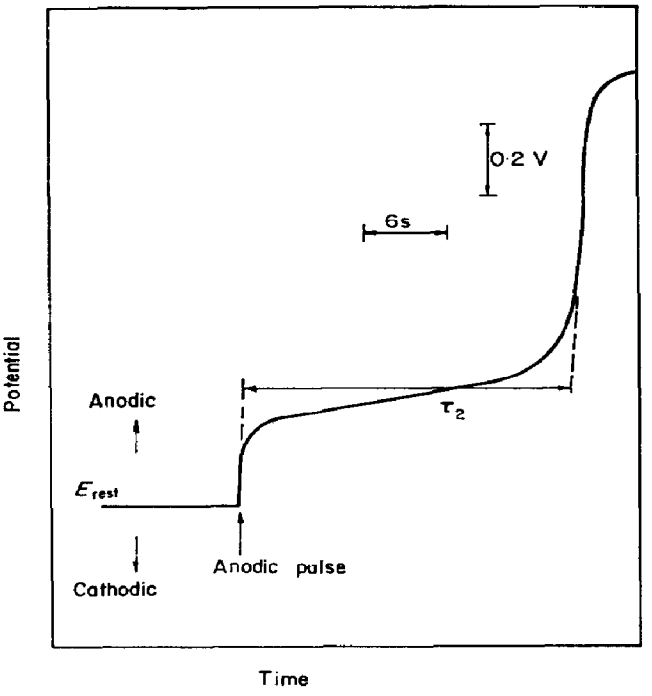

FIG. 13. Time dependence of the electrode potential when an anodic current pulse is applied.
2 M KSCN solution, 162°C.

TABLE 3. PARAMETERS DERIVED FROM GALVANOSTATIC REVERSE PULSE EXPERIMENTS. 27°C, 2 M KSCN

I_a mA	Q_a mC	I_c mA	τ_1 s	τ_2 s	$(I_c\tau_1^{1/2}/Q_a) \times 10^2$ $s^{-1/2}$	$I_c\{[(\tau_1+\tau_2)^{1/2} - \tau_1^{1/2}]/Q_a\} \times 10^2$ $s^{-1/2}$
0·24	7·43	0·23	2·10	5·01	4·50	3·77
0·24	5·63	0·23	1·95	3·90	7·83	4·18
0·41	11·7	0·41	2·01	3·60	4·98	3·32
0·70	16·8	0·70	2·40	2·64	6·45	2·89
0·70	25·2	0·70	3·00	3·60	4·82	2·32
1·00	36·0	1·00	3·60	3·60	5·26	2·19
1·00	28·9	1·00	3·00	1·91	6·00	1·66
1·30	23·4	1·30	2·10	1·80	8·06	2·92
1·30	41·3	1·30	3·21	3·00	5·60	2·23
					Mean 5·94 ± 1·9	Mean 2·83 ± 1·3

$\langle E_{\tau_1/4} - E_{rest}\rangle = 0{\cdot}45$ V
$\langle E_{\tau_2/4} - E_{rest}\rangle = -0{\cdot}38$ V

TABLE 4. PARAMETERS OBTAINED FROM REVERSE PULSE GALVANOSTATIC EXPERIMENTS 70°C, 2 M KSCN

I_a mA	Q_a mC	I_c mA	τ_2 s	$(I_c\tau_2^{1/2}/Q_a) \times 10^2$ $s^{-1/2}$
0·40	30·0	0·40	5·19	3·04
0·69	33·1	0·69	3·75	4·03
1·14	51·3	1·14	3·90	4·39
1·68	70·5	1·68	5·22	5·44
$E_{\tau_2/4} - E_{rest} = -0{\cdot}12$ V				Mean 4·23 ± 1·2

630 and 1200 mC/cm². No transition times during the cathodic pulse were observed during these runs, and the insoluble film became detached from the electrode. Results from these experiments are summarized in Table 5. The charge is necessary to passivate the electrode increases with the anodic current.

TABLE 5. PARAMETERS DERIVED FROM GALVANOSTATIC EXPERIMENTS 162°C, 2 M KSCN

I_a mA	τ_a s	$I_a\tau_a$ mC	$i_a\tau_a$ mC/cm²	$E_{\tau_a/2}$ V
3·15	25·2	79·3	630	0·310
3·58	22·4	80·0	637	0·300
4·75	18·7	89·0	703	0·315
5·70	15·8	90·0	715	0·330
7·12	13·4	95·0	752	0·355
9·50	11·2	107	842	0·383
9·50	11·4	108	860	0·378
14·0	9·00	127	1010	0·385
14·2	9·15	130	1030	0·397
14·2	8·85	126	1000	0·385
25·4	5·85	149	1180	0·490

Potentiostatic pulses with concentrated KSCN *solution*

The anodic potentiostatic experiments were made at 175°C with a 2 M KSCN solution, to form an anodic film on the electrode surface. Potentiostatic pulses were

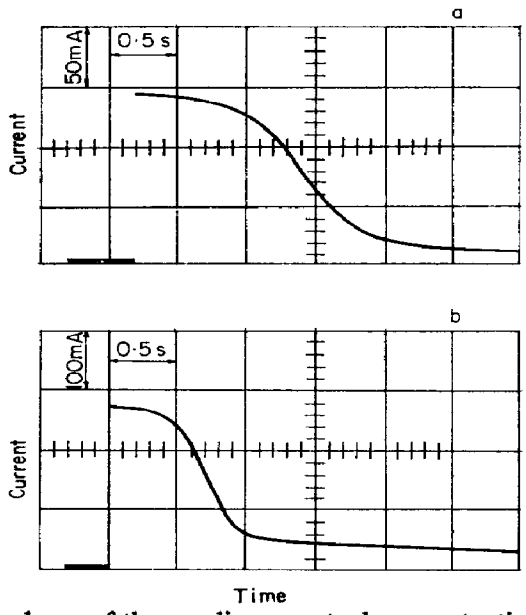

FIG. 14. Time dependence of the anodic current when a potentiostatic pulse is applied. 2 M KSCN solution, 157°C. a, $E - E_{rest} = 1{\cdot}035$ V; b, $E - E_{rest} = 1{\cdot}530$ V.

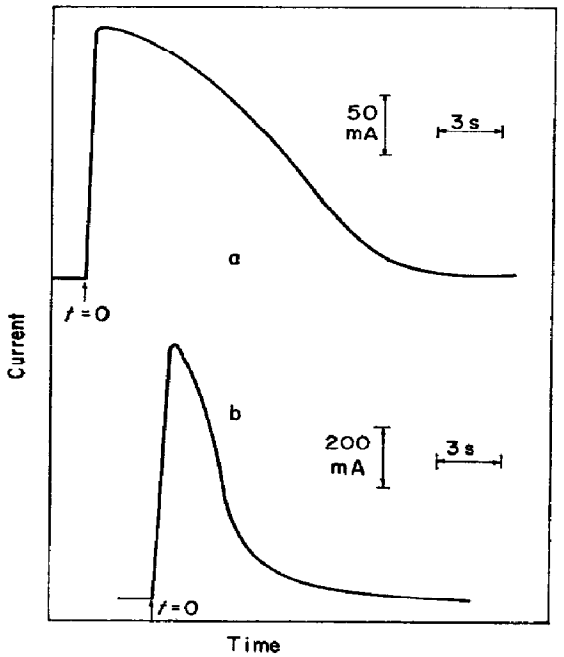

FIG. 15. Time dependence of the anodic current when a potentiostatic pulse is applied. 2 M KSCN solution, 162°C. a, $E - E_{rest} = 0{\cdot}650$ V; b, $E - E_{rest} = 1{\cdot}304$ V.

used from 0·52 up to *ca* 1·5 V, with recording of the current/time curve (Figs. 14 and 15). With an anodic potential pulse, the maximum current is obtained almost instantaneously, decreasing afterwards to zero after a certain time that depends on the potential applied and on the maximum current obtained. In Table 6 the information is shown collected from the current/time records, namely the maximum current, I_m, the potential pulse, E, and the charge Q, during the transient. A linear relationship

TABLE 6. PARAMETERS DEDUCED FROM POTENTIOSTATIC PULSE EXPERIMENTS AT 162°C AND $C_{KSCN} = 2$ M.

E V	$I_m \times 10^3$ A	Q mC	q mC/cm²
0·650	21·8	173	1370
0·780	35·7	209	1659
0·912	49·5	247	1960
0·978	55·5	229	1817
0·978	57·0	246	1952
1·040	63·0	252	2000
1·175	75·0	269	2135
1·304	89·0	266	2111

between the maximum current and the potential applied is obtained (Fig. 16). The slope of the straight line corresponds to a resistance of 9·5 Ω, which coincides with that determined galvanostatically at $t = 0$ from the E/time records.

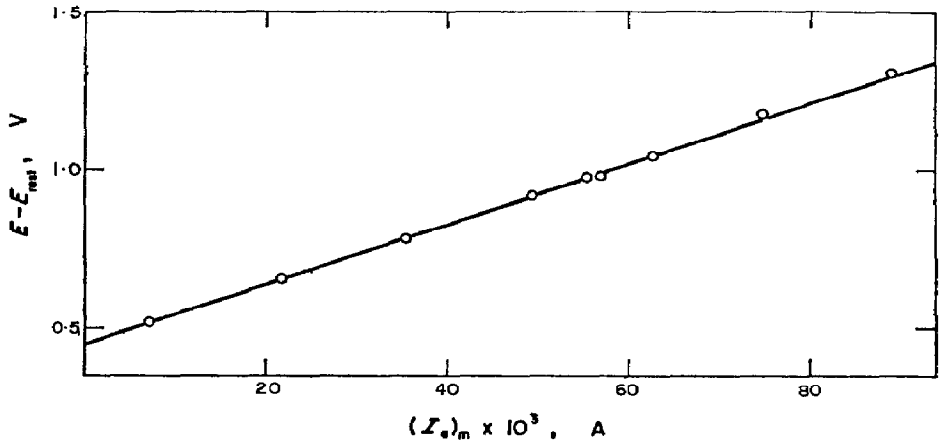

FIG. 16. Dependence of the anodic current maximum with the potential of the applied pulse.
2 M KSCN solution, 162°C.

Anodic E/I curves with solutions of low KSCN *concentration in the presence of supporting electrolyte*

The anodic E/I curves were obtained potentiostatically in the range of 25 to 30°C, using a rotating platinum disk electrode. Figure 17 shows E/I curves obtained with a 10^{-2} M KSCN solution in the presence of 1 M $KClO_4$ at constant rotation speed, ω, the current readings being made at different times. The current decreases as the time increases. The E/I curve obtained when the potential is increased above the rest value, shows an appreciable current only when an overpotential of 0·7 V is applied. The return curve shows marked hysteresis. A stirring effect on current is observed beyond 1·5 V (Fig. 18).

Over a wide region of the E/I curve, there is no effect of rotation speed of the electrode on the current. The semilogarithmic plot of the first part of the curve

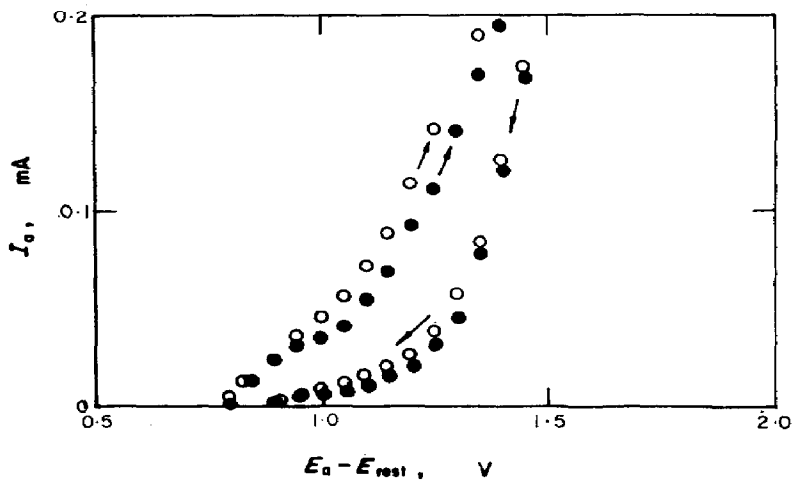

FIG. 17. Potentiostatic E/I curves obtained at 639 rev/min. 0·01 M KSCN + 1 M $KClO_4$ solution, 30°C. ○, current readings each 30 s; ●, current readings each 60 s.

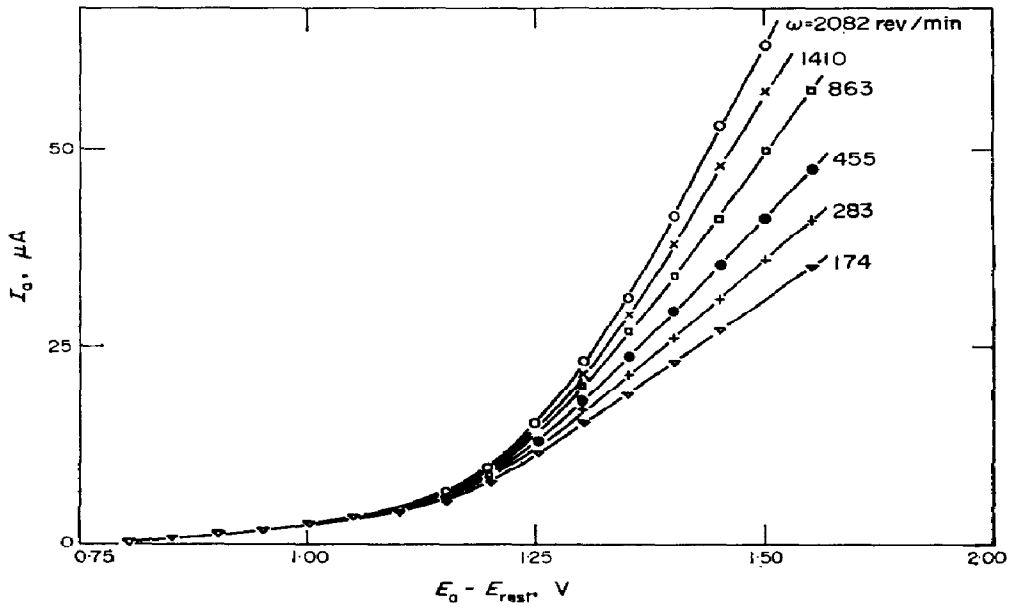

FIG. 18. Potentiostatic anodic E/I curves obtained at different rotation speeds. 0·002 M KSCN + 1 M $KClO_4$, 30°C.

approaches a slope of the order 0·30 V at 30°C. Within this region the current, at constant potential, is a linear function of $\omega^{1/2}$ (Fig. 19). The current at infinite rotation speed satisfies a Tafel relationship (Fig. 20), without correction for the ohmic resistance, the slope being about 0·30 V at 30°C (Fig. 21), as was deduced before. These results show that an irreversible electrochemical reaction occurs at low overpotentials, producing a considerable modification of the electrode surface, so that I_a decreases with time at constant potential.

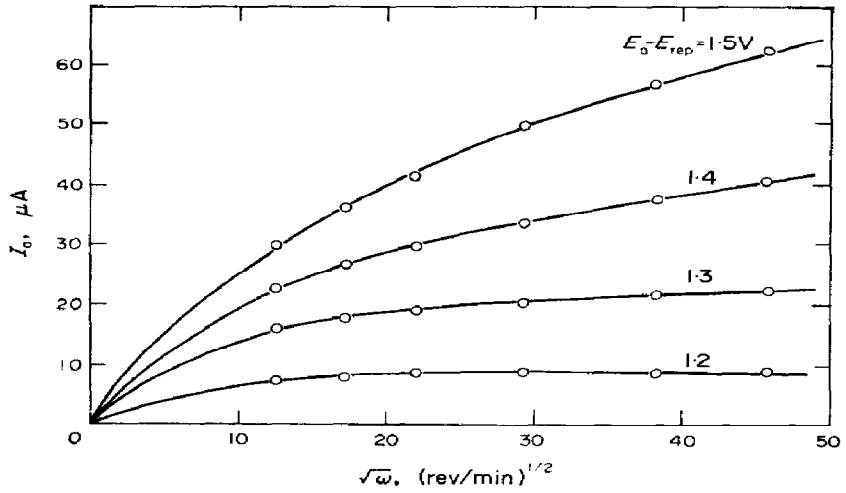

FIG. 19. Dependence of the anodic current on the rotation speed of the electrode at various constant potentials. Data taken from Fig. 18.

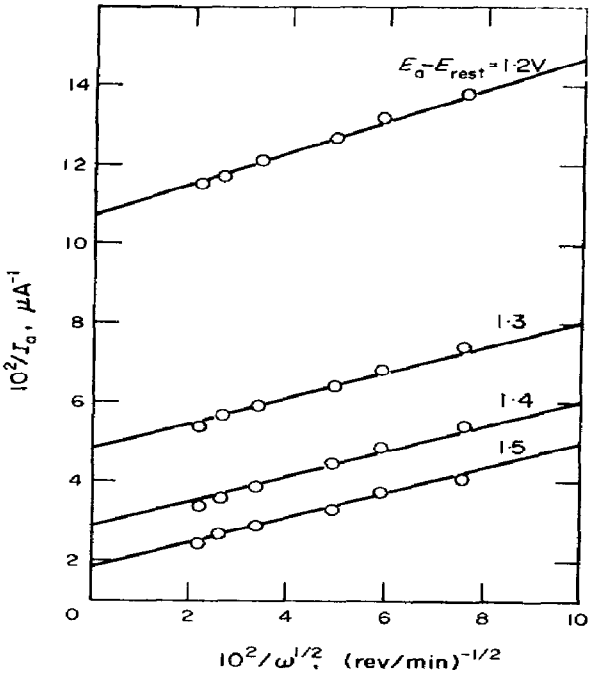

FIG. 20. Plots of $1/I$ *vs.* $1/\omega^{1/2}$ at different potentials. Data taken from Fig. 18.

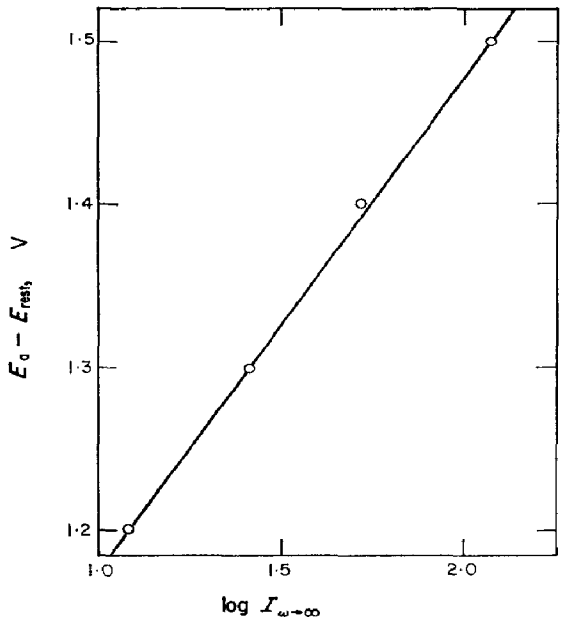

FIG. 21. Tafel plot made with data taken from Fig. 20.

Cathodic E/I curves with low KSCN *concentration in the presence of supporting electrolyte previously anodically electrolysed*

These experiments were attempted to study the electrochemical kinetics of the reactions involving the participation of the more stable substance formed as a consequence of the anodic oxidation of SCN^- ion. As described for cyclic voltammetry, when a solution of KSCN is electrolysed at room temperature, the anodic reaction yields a substance that may subsequently be reduced cathodically at potentials between −0·35 and −0·9 V with respect to the rest potential. To determine the faradaic yields for the formation of the substance a 2×10^{-2} M KSCN in 1 M $KClO_4$ solution was electrolysed at an anodic overvoltage of 0·15 V, using an electrolytic cell with separated compartments and a silver coulometer. Previous to the anodic electrolysis, the cathodic *E/I* curve was determined to confirm the absence of the substance before anodic electrolysis. Between 0 and −1 V, the residual cathodic current was of the order 0·18 μA and at −1·5 V it reached only 2 μA.

The solution treated anodically at 30°C for a certain time was then cathodically electrolysed with a platinum rotating disk electrode. The *E/I* curves (Fig. 22) exhibit a limiting current, I_L, in the potential range between −0·5 and −1 V. The height of the cathodic wave depends linearly on $\omega^{1/2}$ (Fig. 23). The potential region related to the limiting current narrows as the rotation speed is increased. If a second anodic experiment is made with the same solution, to accumulate reaction product, and then a new cathodic curve is obtained, the latter keeps its essential characteristics (Fig. 22).

At constant ω, the limiting current increases proportionally to the concentration of the accumulated substance(s) (Fig. 23). The ratio of the limiting currents in two successive experiments is 1·2 as is to be expected from the silver quantities deposited

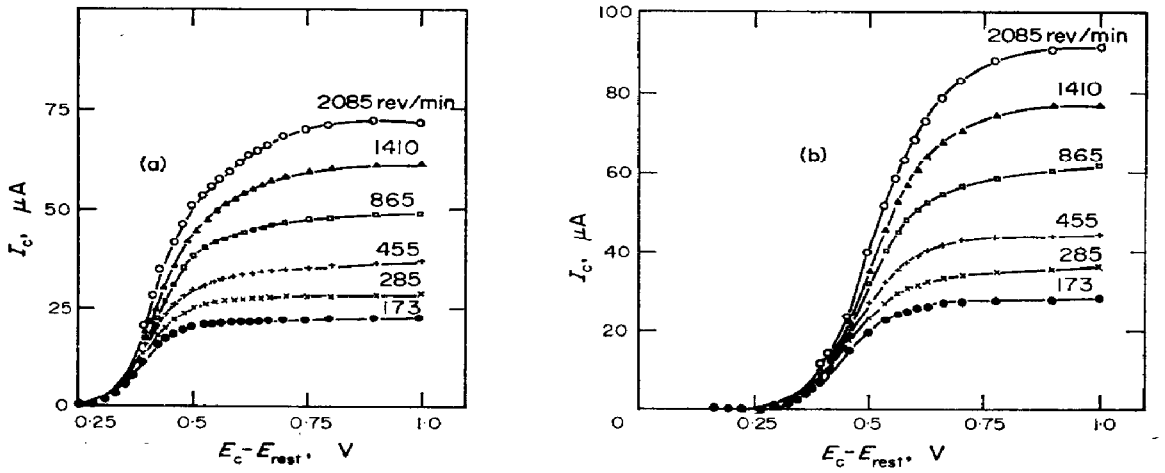

FIG. 22. Cathodic E/I curves recorded at different rotation speeds. Reduction of the stable substance formed during the anodic reaction.
0·002 M KSCN + 1 M $KClO_4$, 30°C. a, quantity of product accumulated equivalent to 0·0637 g Ag; b, quantity of product accumulated equivalent to 0·0762 g Ag.

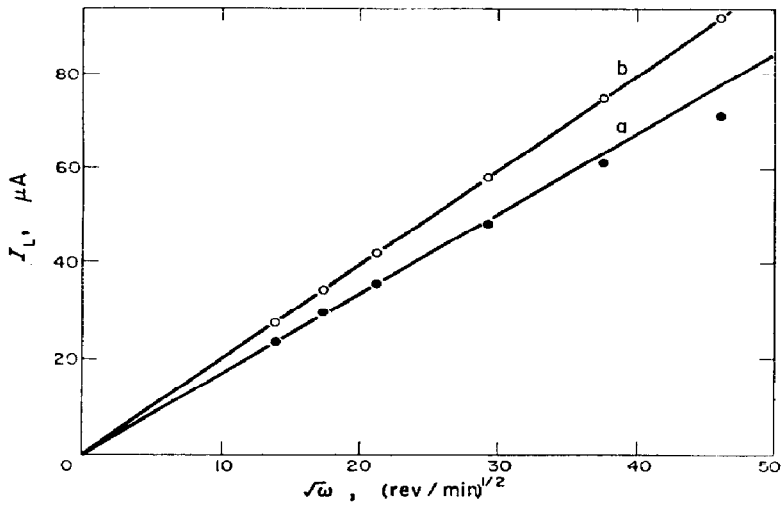

FIG. 23. Relationship between the cathodic limiting current and rotation speed of the working electrode. Conditions as in Fig. 22.

in the two anodic electrolyses. The cathodic E/I curve shows, between 0·4 and 0·5 V, the behaviour of a reaction controlled by 'intermediate' kinetics. To separate the contributions of the activated process from the convective diffusion process, assuming the former to be a first order electrochemical process, $1/I$ is plotted as a function of $1/\omega^{1/2}$ at constant potential (Fig. 24). The extrapolated current at $\omega \rightarrow \infty$ depends on potential according to a Tafel equation (Fig. 25). The Tafel slopes at 30°C are between 0·130 and 0·145 V/decade. The E/I curves also show that the half-wave cathodic potential, $(E_{1/2})_c$, shifts towards more negative values as ω increases, Fig. 26; a linear relationship appears between $(E_{1/2})_c$ and log $\omega^{1/2}$ with a slope of 0·133 V/decade at 30°C.

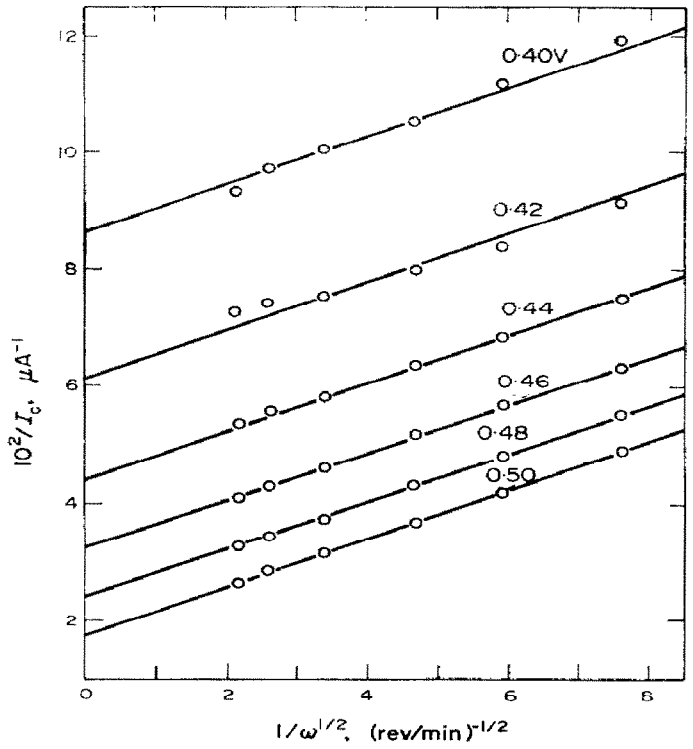

FIG. 24. Plot of $1/I$ *vs* $1/\omega^{1/2}$ at different constant potentials. Data taken from Fig. 22(b).

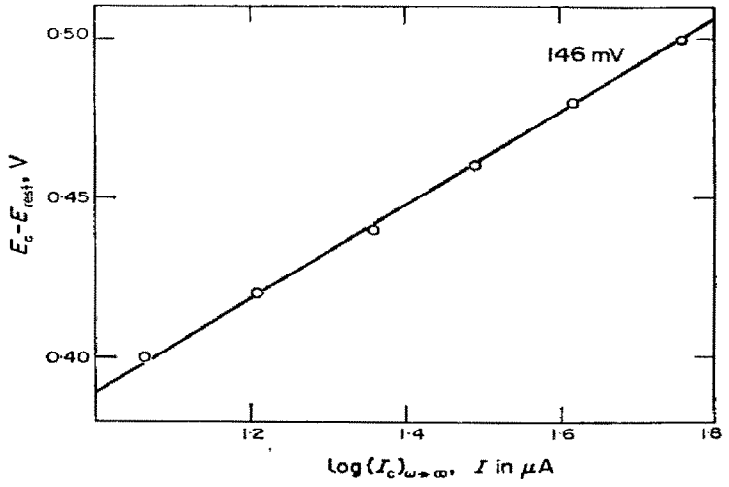

FIG. 25. Tafel plot with data from Fig. 24.

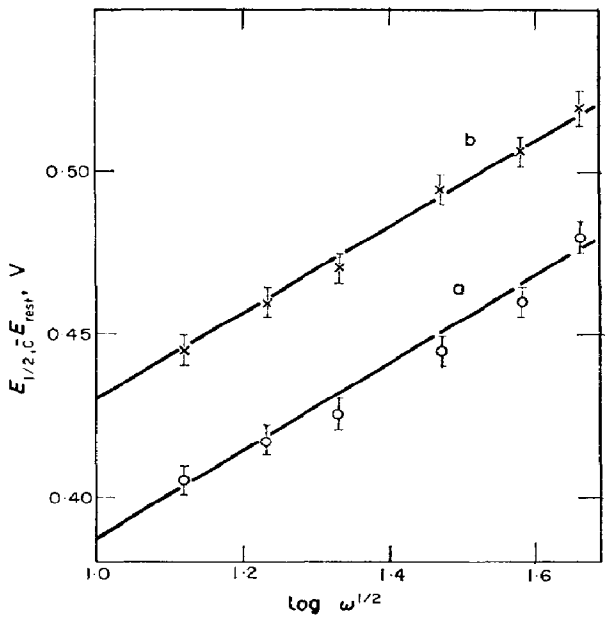

FIG. 26. Dependence of the half-wave potential related to the cathodic reduction of the product formed during the anodic reaction, on the logarithm of the rotation speed of the working electrode. Data from Fig. 22.

INTERPRETATION AND DISCUSSION

The experimental results show clearly the influence of temperature on the anodic and cathodic reactions and, at constant temperature, the coincident behaviour yielded by the different measurements. For a better interpretation and discussion it is convenient to analyse the reactions independently for each temperature range investigated.

The reactions in the 25°C region

The earlier results obtained with solutions of $(NH_4)SCN$ in ACN at temperatures lower than 0°C[5], near the boiling point of the solvent,[6] and also with molten KSCN, facilitate the interpretation of the present results and a discussion of the likely mechanism of the different electrode reactions.

The results at 25°C can be compared to those of the couple $SCN^-/(SCN)_2$ at low temperature in ACN[5]. In that case, a well-defined anodic limiting current was observed with a rotating platinum disk electrode, as well as the corresponding anodic current peak during the increasing half-cycle in cyclic voltammetry. During the increasing half-cycle the current peak related to the cathodic reduction of $(SCN)_2$ was then observed. The two current peaks are located at potentials more positive than the rest potential, and their potential difference is, at 10 mV/s, 0·275 V. When these results are compared to the ones reported above for DMSO solutions, some similarities are observed, such as the tendency of the appearance of an anodic current peak at potential sweep rates higher than 20 mV/s, and the complementary cathodic current peak. The two reactions take place at positive potentials with respect to the rest potential and their difference is of the order 0·250 V. In consequence, during the anodic discharge of the SCN^- ion in DMSO the redox couple $(SCN)_2/SCN^-$ is produced at 25–30°C,

although the system at this temperature is unstable, and therefore the over-all reaction more complicated, as shown by the occurrence of two cathodic current peaks in separated potential zones. At potentials more negative than the rest potential the reduction of a compound more stable than $(SCN)_2$ takes place, this compound having being produced by the anodic reaction.

The preceding facts suggest that the anodic oxidation of the SCN^- ion begins with a charge-transfer reaction,

$$SCN^- + Pt \rightarrow Pt(SCN) + e. \tag{1}$$

The intermediate SCN, adsorbed on the electrode, yields, at least in part, $(SCN)_2$, either by

$$2\,(SCN)Pt \rightarrow (SCN)_2 + 2\,Pt \tag{2}$$

or by means of a second charge-transfer process,

$$(SCN)Pt + SCN^- \rightarrow (SCN)_2 + Pt + e. \tag{3}$$

At room temperature $(SCN)_2$ is unstable and consequently it may react either with DMSO molecules, with another (SCN) radical or with H_2O molecules. In the first case the possible over-all reactions may be written:

$$(SCN)_2 + (CH_3)_2SO = (SCN)H_2CSOCH_3 + H^+ + CN^- + S, \tag{4}$$

and

$$\left.\begin{aligned}(SCN)Pt + (CH_3)_2SO &= R + H^+ + CN^- + S,\\ R &\rightarrow \text{Products},\end{aligned}\right\} \tag{5}$$

where R is an organic radical. The second possibility is expressed by

$$(SCN)_2 + 4\,H_2O \rightarrow SO_4^{2-} + 2\,HCN + 6\,H^+ + S + 4\,e, \tag{6}$$

and

$$(SCN)Pt + 4\,H_2O = SO_4^{2-} + HCN + 7\,H^+ + Pt + 5\,e. \tag{7}$$

The over-all reaction for the third possibility can be expressed

$$x(SCN)_2 \rightarrow (SCN)_{2x}. \tag{8}$$

Reactions (4) to (7) are equivalent to those which are produced by chlorine in DMSO[12] and are to be expected if the redox couple $(SCN)_2/SCN^-$ acts as a pseudo-halogen electrode closely resembling the chlorine electrode.[5] The radical (SCN) may be considered equivalent to a halogen atom. Reaction (8) is the polymerization of the thiocyanogen to parathiocyanogen, which cannot be reduced electrochemically at low temperature. Consequently if any of the reactions (4) to (7) occurs, a cathodic current related to the discharge of the hydrogen solvated ion should be observed. The potential region for this reaction for the hydrogen halides dissolved in aprotic solvents, with respect to the discharge potential of the halogen ions, lies at 0·8 V towards the negative side.[13] This is approximately the potential difference observed between the potential where the reduction of the $(SCN)_2$ begins (within a few mV of the reversible potential of the couple $(SCN)_2/SCN^-$)[5] and that of the cathodic current peak. The former is located a few mV more negatively than the reversible potential of the $(SCN)_2/SCN^-$ couple, and the latter is negative to the rest potential.

The two cathodic current peaks show a potential difference similar to that observed in the galvanostatic experiments at low temperature. The cathodic transition times fulfil satisfactorily the $i\tau^{1/2}$ = constant relationship. This indicates that the sudden change of the potential at the reaction interface corresponds to the depletion of the reactant species. The existence of different competitive reactions for the product of the initial discharge of the thiocyanate ion explains the following facts: (i) the existence of the $(SCN)_2$ current reduction only in transients measured at low temperatures; (ii) its disappearance at 60 and 160°C; (iii) the occurrence of a cathodic current related to the discharge of the solvated hydrogen ion; (iv) the competition between the reaction yielding the solvated hydrogen ion and the formation of the polymer, with the second prevailing over the first at high temperatures. In consequence at 27°C it becomes clear that the electrochemical reaction associated with SCN^--ion discharge in DMSO is more complicated than that observed in ACN at lower temperatures, although the charge-transfer processes are equivalent.

Possible mechanism of the anodic reaction at low temperature

The experiment shown in Fig. 17 exhibits a hysteresis in the *E/I* curve opposite of that obtained in the cyclic voltammetry and the effect is associated with the duration of each experiment. As the time of residence of the electrode at a fixed potential increases, as in the experiment of Fig. 17, passivity onset is much easier. This shows that the polymerization reaction takes place even at low temperature, as has been observed also with solutions of KSCN in ACN.[5]

Figures 18 and 19 indicate a mixed control kinetics in the oxidation of the SCN^- ion at low temperature, between 1·2 and 1·5 V. At potentials lower than 1·2 V the total reaction is practically independent of the rotation speed of the working electrode, being afterwards controlled by the rate of the electrochemical reaction. At potentials higher than 1·5 V, there is a tendency to get, at constant potential, a linear relationship between I and $\omega^{1/2}$, characteristic of electrode processes under convective-diffusion control. The corresponding limiting current is not easily defined because of the interference of the polymerization reaction. The Tafel slope for the activated process (Fig. 21) is of the order of 0·3 V/decade, a value which is compatible with the existence of a slow charge transfer plus an appreciable polarization contribution due to the non-conducting film formed on the electrode.

Two possible reaction mechanisms (I and II) can be postulated to explain this process.

Mechanism I:

$$SCN^- + Pt \xrightarrow{rds} (SCN)Pt + e, \qquad \text{(Ia)}$$

$$2\,(SCN)Pt \rightleftarrows (SCN)_2 + 2\,Pt. \qquad \text{(Ib)}$$

Mechanism II:

$$SCN^- + Pt \rightleftarrows (SCN)Pt + e, \qquad \text{(IIa)}$$

$$(SCN)Pt + SCN^- \xrightarrow{rds} (SCN)_2 + Pt(e), \qquad \text{(IIb)}$$

where rds means rate-determining step. Supposing that the adsorption of the reaction intermediate follows a Langmuir isotherm, these two mechanisms explain the kinetic behaviour of the $(SCN)_2/SCN^-$ electrode in ACN at low temperature.[5] Mechanism II has been postulated for the halogen electrodes in aprotic solvents.[14–16] Mechanism II also takes into account the reverse hysteresis shown in the rapidly recorded *E/I* curves.

The effect may be due to a transitory accumulation of the reaction intermediates on the electrode surface.

Probable mechanism of the cathodic reactions at low temperature

The products formed during SCN^--ion discharge are responsible for the appearance of reduction currents. The first current, at potentials positive with respect to the rest potential, is evidenced in the cyclic voltammetry runs; its maximum shifts towards more negative potentials when the potential-sweep rate is increased. This behaviour is consistent with that expected for the reduction of the $(SCN)_2$, whose kinetics would be controlled by a charge-transfer step, as occurs for the same reaction in ACN.[5] Reactions I or II in the reverse direction may be useful for explaining the reduction of $(SCN)_2$. The other reaction product formed is stable, it accumulates in the solution, and it is still obtained at an intermediate temperature; its discharge potential coincides with that for hydrogen-ion discharge.[17,18] Besides, both the Tafel slope and the dependence of the half-wave potential on the rotation speed as well as the cathodic current peak shift with the potential-sweep rate, agree with the discharge of the hydrogen ion in aprotic solvents. In consequence, the measured kinetic parameters can easily be explained in accordance to the well-known mechanisms for the hydrogen-ion discharge as indicated further on, supposing that the hydrogen atom adsorption on the platinum follows a Langmuir isotherm,

Mechanism III:

$$(H^+)_{solv} + Pt(e) \xrightarrow{rds} (H)Pt, \qquad \text{(IIIa)}$$

$$2\,(H)Pt \rightleftarrows 2\,H_2 + 2\,Pt. \qquad \text{(IIIb)}$$

Mechanism IV:

$$(H^+)_{solv} + Pt(e) \rightleftarrows (H)Pt, \qquad \text{(IVa)}$$

$$(H)Pt + (H^+)_{solv} + Pt(e) \xrightarrow{rds} H_2 + 2Pt. \qquad \text{(IVb)}$$

The kinetic analysis of mechanism III with the step IIIa rate-determining and of mechanism IV with step IVb rate-determining, takes into account the experimental Tafel slope of $2RT/F$.

The reactions at ca 60°C

In the intermediate temperature region, the disappearance of the cathodic current related to the reduction of $(SCN)_2$ is observed. The discharge of the SCN^- ion occurs at a lower potential and the same happens with the reduction of the hydrogen ion. These facts are observed both in the voltammetric curves and in the galvanostatic runs. The temperature increase produces a hysteresis in the E/I curve (Fig. 3) contrary to that observed at room temperature, showing that film formation is much favoured in these circumstances. Nevertheless everything occurs as if a total blockage of the electrode surface is not produced. The over-all kinetic behaviour at these temperatures is consistent with the reactions already discussed.

The anodic reaction at 162°C

At 162°C the SCN^--ion oxidation reaction yields the formation of a $(SCN)_x$ film which causes the passivation of the electrode by blocking its surface. At these temperatures the oxidation reaction occurs at a lower potential than in the cases previously considered. The galvanostatic runs showed the non-existence of a constant product

$I\tau^{1/2}$. Instead, the product $I\tau$ increases with the current, which is consistent with film formation on the electrode. The values of $E_{1/2}$ and Q_a obtained galvanostatically and potentiostically also increase with the current. From the Q_a values it can be deduced that the average film thicknesses are between $1{\cdot}5 \times 10^{-4}$ cm and $6{\cdot}5 \times 10^{-4}$ cm, if the apparent specific gravity of the film[8,9] is taken as 2·0 g/cm³. These thicknesses indicate that the film, in terms of $(SCN)_2$ units, is formed by an appreciable number of molecular layers.

Kinetics of the electrochemical formation of parathiocyanogen

The results show that the film formation is related to an ohmic and to a non-ohmic polarization contribution. If the reaction were exclusively controlled by an ohmic resistance, its kinetics would be explained by the Müller model,[19] which distinguishes two principal stages in film formation. There is first a superficial growth at constant thickness until there are only pores of small diameter, and afterwards growth of the film thickness at constant porosity. The current transient related to the superficial film growth at constant potential is given by

$$t = \tau^* + A\left[\frac{-1}{I_I - I} + \frac{1}{I_I}\ln\left(\frac{I_I - I}{I}\right)\right], \tag{9}$$

where I_I is the total current which corresponds to the asymptote at the origin of the I/t curve; τ^* and A are two constants to be calculated from the transient; τ^* is a measure of the current plateau duration and A is inversely related to the current-increasing rate at the end of the plateau. Equation (9) did not fulfill the experimental results at large values of t (Fig. 27). This shows an additional kinetic contribution not comprised in the Müller model.

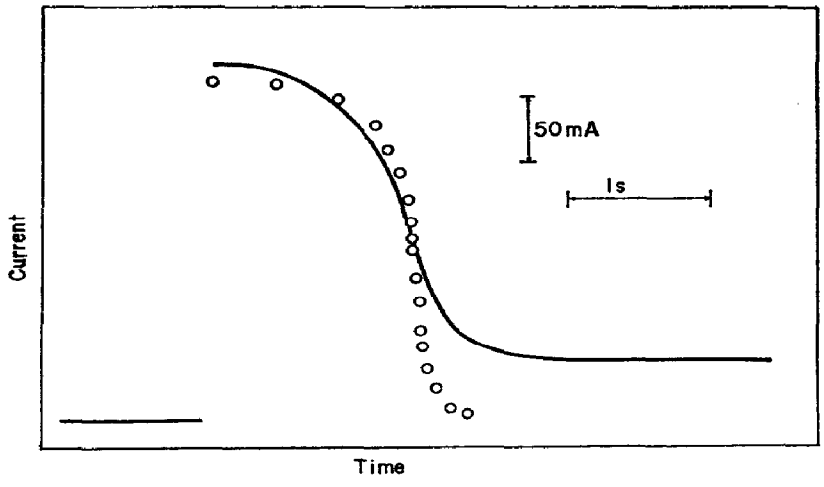

FIG. 27. Comparison of a current/time record (at 1·53 V) with results given by equation (9) (open circles).

Analysis of voltammetric curves measured with compensation for ohmic resistance (Figs. 7 and 8) allows us to distinguish two regions in the voltagram, one located at lower potentials than that of the current peak and the other at higher . To calculate the theoretical voltagram, the equations deduced for an electrochemical process in

which the initial charge-transfer yields an intermediate able to passivate the reaction surface,[8,20] have been used,

$$-\ln(1-\theta) = K\left\{\exp\left[\frac{\beta vtF}{RT}\right] - 1\right\}, \tag{10}$$

where θ is the degree of surface coverage, K a constant that depends on specific rate constant, on the Tafel slope, on the potential-sweep rate and on the initial potential, β the symmetry factor, and the rest of the terms have then usual significance. If $E - E_{rest}$ is plotted as a function of ln [ln (1/1 − θ)] at potential lower than the anodic current peak potential according to (10), a linear relationship with a Tafel slope of $2RT/3F$ is obtained, Fig. 28. At higher potentials the slope of the straight line increases and it cannot be directly related to the mechanism of reaction. In consequence, the electrochemical reaction, at potentials lower than the anodic current peak potential is slow and in this case the reaction kinetics can be explained only by means of mechanism II, as this mechanism under Langmiur conditions leads to a Tafel slope of $2/3(RT/F)$ at low coverage. This condition must be fulfilled at potentials lower than that of the current peaks. Then the electrode surface seems to act as a quasi-homogeneous surface covered by solvent molecules and the superfical concentration of the nucleation centres, which are of kinetic importance, is low. If the solvent were absent, the mechanism would change, as when the reaction occurs in molten KSCN, because the surface concentration of the nucleation centres is then much larger. The kinetics of the reaction is characterized by another Tafel slope, which implies a different mechanism.[7,8]

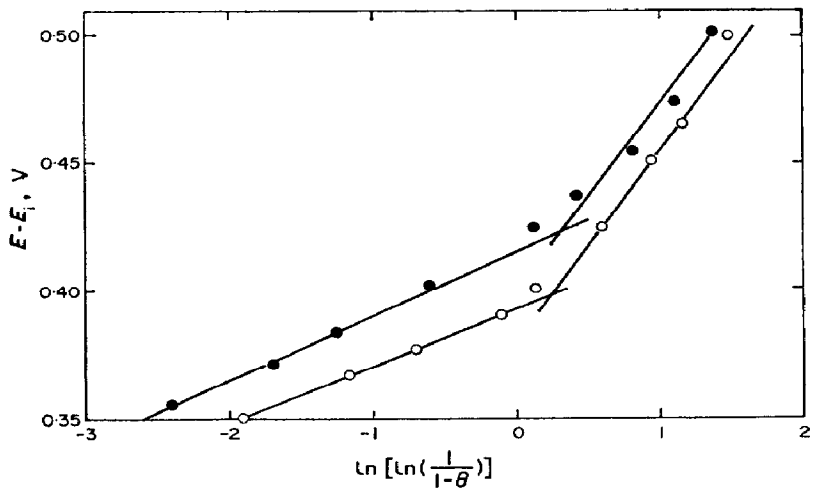

FIG. 28. Plot of $E - E_{rest}$ as a function of ln [ln (1/1 − θ)].
●, 2 M KSCN, electrode area 0·126 cm², v = 5 mV/s, 157°C; ○, 4 M KSCN, electrode area 0·0628 cm², v = 15 mV/s, 152°C.

The results obtained with equation (10) are consistent with those of Fig. 10. The plot of $E - E_{rest}$ *vs* log v shows, at low potential-sweep rates, the same slope $2RT/3F$ within the experimental error. In Figs. 29 and 30 two experimental voltammetric curves are compared with theoretical curves calculated with Tafel slopes of $2RT/3F$ and to $2RT/F$ respectively. It is quite clear that at any sweep rate and at potentials

lower than the anodic current peak potential, the theoretical curve with the first slope reproduces satisfactorily the experimental curve. The slope $2RT/F$ must be discarded. In consequence, this reaction model explains the behaviour of the system as given by the different relationship between the kinetic parameters derived from the cyclic voltammetry.

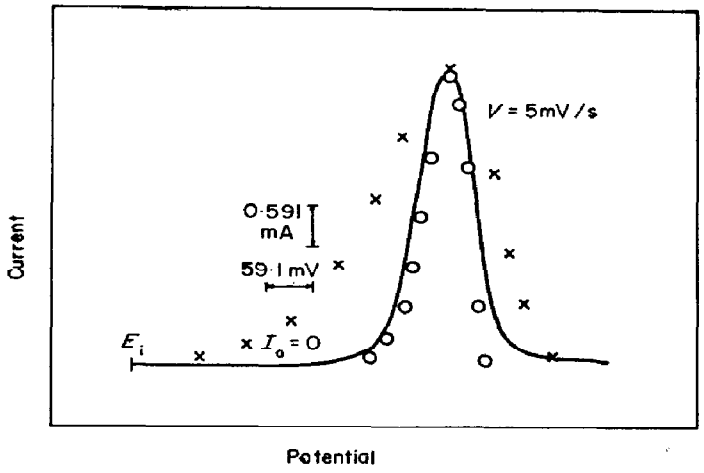

FIG. 29. Voltagram obtained at 5 mV/s with a 2 M KSCN solution at 157°C on a 0·126 cm^2 electrode. ○, data calculated with the slope $2RT/3F$; ×, data calculated with the slope $2RT/F$.

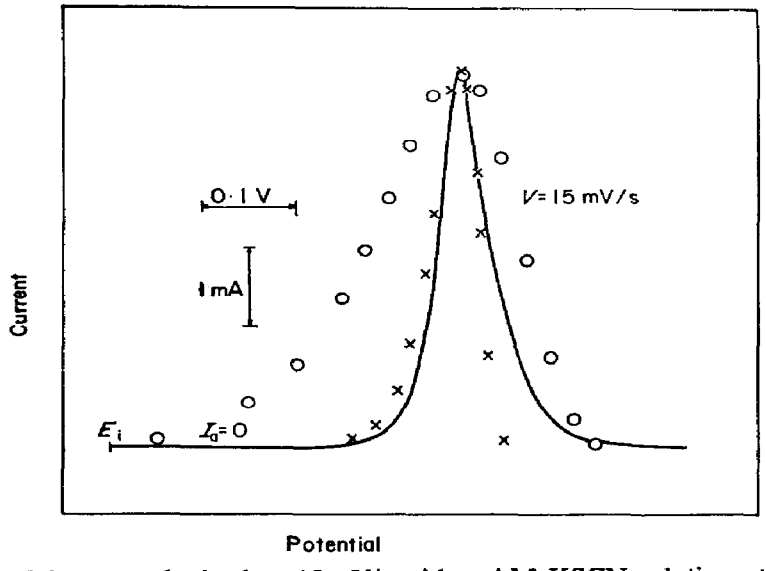

FIG. 30. Voltagram obtained at 15 mV/s with a 4 M KSCN solution at 152°C on a 0·0628 cm^2 electrode.
○, data calculated with slope $2RT/F$; ×, data calculated with slope $2RT/3F$.

Another important fact is that the charge required completely to passivate the electrode increases with the current used or with the potential-sweep rate. This indicates that before the formation of a uniform non-conducting film, the initial patches

have thickened in the direction normal to the electrode surface before getting into lateral touch. That is why nucleation and two-dimensional growth of the nuclei occur preferentially at low potentials (short times), and three-dimensional growth predominates at higher potentials (longer times). A more significant three-dimensional growth takes place at larger potential-sweep rates.

To explain the phenomena that produce the three-dimensional growth of $(SCN)_x$ patches it is convenient to refer to the E/I voltammetric curves recorded at higher potential-sweep rates. For these (Fig. 31), at potentials more positive than those which correspond to the anodic current peak, I decays linearly with $t^{1/2}$. This, together with the growth of the film thickness, shows that the kinetic model is not completely adequate at higher potentials. The large apparent Tafel slope obtained in this region must be considered as the result of the kinetic model already mentioned plus a diffusional contribution to the film growth. These results suggest, therefore, that a more general model for this type of electrochemical processes is needed. This model, in addition to the ohmic contribution given by the Müller model, and the kinetic contribution explained above, should also consider the following aspects: (1) the initial two-dimensional growth; (ii) the steric effect of the solvent in the interphase, which impedes the two-dimensional film growth; (iii) the subsequent three-dimensional growth; (iv) the influence of the potential-sweep rate on the increase of the three-dimensional growth; (v) the diffusion and depletion of the ionic species inside the pores in the growing film; and finally (vi) film-sealing, provoking a partial squeeze-out of solvent or its occlusion inside the film.

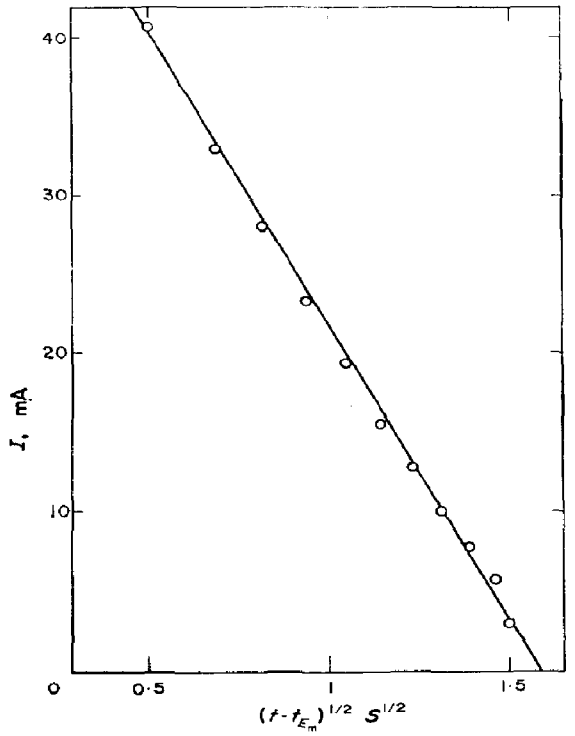

FIG. 31. Time dependence of the anodic current at potential higher than the potential corresponding to the anodic current peak. Data taken from Fig. 8 at 170 mV/s.

Data collected in this work, together with the experiments made in ACN[5,6] and in molten KSCN,[7,8] indicate the participation of the various steps mentioned above. Quantitative presentation of the model will be possible once additional kinetic information is obtained, especially data related to the temperature effect on the different stages of the possible reaction mechanisms.

Acknowledgements—This work is part of the research program of the INIFTA, which is sponsored by the Universidad Nacional de La Plata, the Consejo Nacional de Investigaciones Científicas y Técnicas and by the Comisión de Investigaciones Científicas de Buenos Aires. C. M. thanks the Universidad Nacional de Tucumán for the fellowship granted during 1969 and 1970.

REFERENCES

1. R. Gaugin, *Ann. Chim.* **4**, 832 (1949).
2. O. A. Songina and I. M. Pavlova, *Izv. Vysskikh. Ucheb. Zavedenii Khim. i Khim. Teckhnol.* **5**, 378 (1962).
3. M. M. Nicholson, *Anal. Chem.* **31**, 128 (1959).
4. A. P. Tomilov, *Russ. Chem. Rev.* **30**, 369 (1961).
5. G. Cauquis and G. Pierre, *C.r. Acad. Sci., Paris* **266**, 883 (1968).
6. R. Pereiro, A. J. Arvía and A. J. Calandra, *Electrochim. Acta* **17**, 1723 (1972).
7. R. Pereiro, A. J. Arvía and A. J. Calandra, in preparation.
8. A. J. Calandra, M. E. Martins and A. J. Arvía, *Electrochim. Acta*, **16**, 2057 (1971).
9. A. J. Arvía, A. J. Calandra and M. E. Martins, *Electrochim. Acta*, **17**, 741 (1972).
10. J. Wargon and A. J. Arvía, *Electrochim. Acta*, **16**, 1619 (1971).
11. G. Paus, A. J. Calandra and A. J. Arvía, *An. Soc. Cient. Arg.* **192**, 35 (1971).
12. H. E. Zittel and F. J. Miller, *Anal. Chim. Acta* **37**, 141 (1967).
13. M. Michlmayr and D. T. Sawyer, *J. electroanal. Chem.* **23**, 387 (1969).
14. A. J. Arvía, M. C. Giordano and J. J. Podestá, *Electrochim. Acta* **14**, 389 (1969).
15. T. Iwasita and M. C. Giordano, *Electrochim. Acta* **14**, 1045 (1969).
16. L. Sereno, V. A. Macagno and M. C. Giordano, *Electrochim. Acta* **17**, 561 (1972).
17. J. A. Olabe and A. J. Arvía, *Electrochim. Acta* **14**, 785 (1969).
18. J. A. Olabe and A. J. Arvía, *Electrochim. Acta* **15**, 1685 (1970).
19. W. J. Müller, *Trans. Faraday Soc.* **27**, 737 (1931).
20. E. Gileadi and S. Srinivasan, *Electrochim. Acta* **11**, 321 (1966).